Macromolecules

ARTICLE

pubs.acs.org/Macromolecules

Fractal Structures from Amphiphilic Random Azo Copolymer

Nan Li, Yaobang Li, and Xiaogong Wang*

Department of Chemical Engineering, Laboratory for Advanced Materials, Tsinghua University, Beijing 100084, P. R. China

Supporting Information

ABSTRACT: This article reports for the first time the observation of a series of fractal structures formed from a representative amphiphilic random azo copolymer (PPAPE). The fractal structures were obtained from colloidal spheres of PPAPE through aggregation and structural reorganization in aqueous dispersions. In the process, the colloidal spheres with hydrophobic cores were first prepared by gradual hydrophobic aggregation of PPAPE in H_2O/THF medium with a continuous increase in the water content. The fractal structures were then obtained by gradually adding an aqueous solution of NaOH (0.2 M) into the weakly acidic dispersions of the colloidal spheres to different pH values. The fractal aggregates were investigated by transmission electron microscopy (TEM), scanning electron microscopy (SEM), static light scattering (SLS), and dynamic light scattering (DLS). Photoisomerization behavior of the azobenzene units was investigated to detect the local environment around the molecular probes in the aggregates. The results show that by adjusting the pH of the dispersions to different values (from 8.2 to 11.7), fractal aggregates with different morphology and fractal dimensions (d_f) are obtained. At low pH side (pH = 8.2), the fractal structures are formed from partially dissociated colloidal spheres with d_f of 1.68 ± 0.03, which corresponds to a diffusion-limited cluster aggregation (DLCA) process. When pH is 9.4, the fractal aggregates are built up with fine needle-shaped branches with size as small as 10−20 nm and d_f is measured to be 2.14 ± 0.03, which is similar to a reaction-limited cluster aggregation (RLCA) case. For the high pH (pH = 11.7), the fractal dimension increases to 2.24 ± 0.02 and fractals appear as denser aggregates. The photoisomerization study shows that the fractal structures possess a relatively loose inner structure compared to the initial colloidal spheres. The observations suggest that the well-organized fractal structures obtained in the high-pH dispersions are formed by the aggregation of partially dissociated colloidal spheres and the subsequent structural reorganization at the molecular level. The understanding of the molecular self-assembling process can be used to develop photoresponsive materials with fractal architecture for future applications.

1. INTRODUCTION

Polymers containing azobenzene and its derivatives (azo polymers for short) have aroused considerable research interest in the past decades.[1−3] The reversible trans−cis photoisomerization feature of azobenzenes endows azo polymers a variety of photoresponsive properties such as photoinduced phase transition,[4] chromophore orientation,[5] photomechanical bending or rotation,[6,7] and surface-relief-grating (SRG) formation.[8] Polymers with such properties can be used in the areas of photoswitching, optical data storage, light-triggered reactors, microactuators, sensors, and artificial muscles among others.[1−3,9] In recent years, self-assembly of amphiphilic azo polymers has attracted increasing attention.[10] Different supramolecular structures composed of amphiphilic azo polymers, such as spherical micelles, rodlike micelles, bilayer vesicles, nanofibers, and hollow tubes, have been obtained through self-assembling processes.[11−16] The self-assembled structures of azo polymers can undergo structural changes both in solution and in the solid state when triggered by light or other external stimuli. Understanding the self-assembling processes can lead to the development of photoresponsive materials with new functions for future applications.

The term "fractal" was coined by Mandelbrot in 1975 for patterns and structures with self-similarity at different scales.[17] Since then, various fractal phenomena have been discovered and extensively studied in different scientific disciplines.[18−26] Fractal clusters composed of tiny particles such as soot and other building blocks can be observed in a growth process far from thermodynamic equilibrium.[18] Two theoretical models, known as diffusion-limited cluster aggregation (DLCA)[19,20] and reaction-limited cluster aggregation (RLCA),[21,22] have been widely accepted to describe the particle aggregation process. In the DLCA process, the diffusion is the rate-limiting step as there is no repulsive interaction between particles and every collision results in an irreversible sticking. On the other hand, for the RLCA process, the sticking probability is so small that the cluster growth often needs many collisions of the building blocks before they stick together. The structures formed from both processes can be described by scaling law with a coefficient called fractal dimension. The DLCA generally leads to open and loose morphology with a low fractal dimension of 1.7−1.8, and the RLCA usually produces aggregates with a denser morphology with a higher fractal dimension of 2.1−2.2 because the particles have more

Received: May 1, 2011
Revised: September 22, 2011
Published: October 05, 2011

opportunity to penetrate into the growing clusters.[22] For diversified applications, fractal structures have been developed by using different building blocks such as latex particles,[23] gold nanoparticles,[24] silver nanowires,[25] and biomolecules,[26] among many others. The materials developed through fractal organization have many technological potentialities for their unique morphology and desirable properties.[23−26]

Associative polymers can generally refer to macromolecules with attractive groups or "sticker" in the chain structures, such as charged polymers, block copolymers in strongly selective solvents, and polymers with hydrogen bonding.[27] Typically, through the ionic interaction, hydrophobic interaction, and hydrogen bonding, the polymer chain associations will lead to the formation of networks and gels.[27b] On the other hand, fractal aggregates have also been observed from associative polymers under different conditions, such as partially hydrolyzed poly(acrylamide)/calcium(II) complexes,[28] hydrophobically modified alkali soluble emulsion (HASE),[29] and gelatin with Cr^{3+}/COO^{-} complexation in dilute solution.[30] In our previous study, a series of polydispersed amphiphilic azo homopolymers and random copolymers have been synthesized.[16,31] The azo polymers can form uniform colloidal spheres through gradual hydrophobic aggregation of the amphiphilic polymers in an aqueous medium.[16] The colloidal spheres show some interesting photoresponsive properties such as shape deformation and dichroism upon light irradiation.[16a,b] The two-dimensional arrays composed of colloidal spheres can transform to ordered mesoporous films through in situ structure inversion caused by solvent treatment.[16c] Theoretically, both the colloidal spheres of the azo polymers and the associative amphiphilic azo polymers can aggregate under proper conditions to develop fractal structures in dispersions. However, to our knowledge, the observation and study of the fractals of azo polymers have not been reported in the literature yet.

In this paper, we report the observation of a series of fractal structures formed from an amphiphilic random azo copolymer in the aqueous media. The fractal aggregates were formed by aggregation of partially dissociated colloidal spheres and structural reorganization of the clusters, which were induced by gradually increasing pH of the weakly acidic aqueous dispersions. Depending on the pH, fractal structures with different morphology and fractal dimensions were formed in the dispersions through the DLCA or RLCA process. The fractal structures were characterized by transmission electron microscopy (TEM), scanning electron microscopy (SEM), static light scattering (SLS), and dynamic light scattering (DLS) measurements. The photoisomerization behavior of the azobenzene units was used as a tool to provide information on the inner structure of the fractal aggregates. The experimental details, results, and discussion are presented in the following sections.

2. EXPERIMENTAL SECTION

2.1. Materials. Analytical pure tetrahydrofuran (THF) from commercial source was refluxed with cuprous chloride and distilled for dehydration prior to use. Deionized water (resistivity >18 MΩ·cm) was obtained from a Milli-Q water purification system. Other reagents and solvents were used as received without further purification. The synthesis and characterization of poly(2-(4-(phenylazo)phenoxy)ethylacrylate-*co*-acrylic acid) (PPAPE) have been reported in our previous report.[31] The polymer was prepared by the Schotten−Baumann reaction between poly(acryloyl chloride) (PAC) and 2-(4-(phenylazo)phenoxy)ethanol (PAPE), and the unreacted acyl chloride groups were then hydrolyzed to yield the carboxyl groups. The degree of polymerization (DP) of PAC was 325 with a polydispersity index of 1.9 estimated by GPC. The PPAPE sample used in this study had the degree of functionalization (DF) of 49.9%, defined as the percentage of the structure units bearing azo chromophores among the total units. The number-average molecular weight (M_n) and the weight-average molecular weight (M_w) of the sample were estimated to be 6.53×10^4 and 1.24×10^5, respectively.

2.2. Colloidal Sphere Preparation. The colloidal spheres, which were used as the building blocks to assemble the fractal aggregates, were prepared by a method described in our previous paper.[16] In the process, PPAPE was first dissolved in THF to form a homogeneous solution with a concentration of 0.8 mg/mL. Then, the deionized water (1 mL) was added dropwise into the THF solution (1 mL). After the water addition was completed, an excess amount of water (18−19 mL) was added to "quench" the structures formed in the dispersion, and the residual THF was removed by dialyzing against water. The total volume of the dispersion was adjusted to 20 mL by adding a small amount of water. The final dispersion was weakly acidic (pH = 5.2) and contained the colloidal spheres with the concentration of 4.0×10^{-5} g/mL.

2.3. Fractal Aggregate Formation. For the preparation of fractal aggregates, a 0.2 M NaOH aqueous solution was gradually added into the prepared dispersions of colloidal spheres until the pH reached the required values. To study the structural changes in the evolution process as well as the fractal characteristics of the formed aggregates, a series of aqueous dispersions with different pH values were prepared. In the process, different amounts of the 0.2 M NaOH solution were gradually added into 3 mL of the dispersions of colloidal spheres. Each time, 5−30 μL of NaOH solution was added into the dispersions, and then the dispersions were left for 5−10 h to reach the pH stable state. A series of dispersions with pH in range from 5.8 (5 μL) to 11.7 (330 μL) were obtained by this procedure. The dispersions with different pH values were used for photoisomerization investigation, and the aggregates separated from the dispersions were examined by TEM and SEM. The laser light scattering (LLS) measurement was performed on the dispersions to determine the parameters such as the hydrodynamic radius (R_h) and the fractal dimension (d_f). For the LLS measurements of the dispersions, the similar procedure was carried out to obtain fractal aggregates by using dust-free dispersions of PPAPE colloidal spheres and dust-free NaOH aqueous solution. The colloidal sphere dispersions and NaOH aqueous solutions were respectively clarified by a 0.45 and 0.1 μm Millipore filter to remove dust.

2.4. TEM and SEM Characterization. TEM images were obtained by using a JEOL-JEM-1200EX electron microscope with an accelerating voltage of 120 kV. The TEM samples were prepared by casting diluted dispersions onto the copper grids coated with a thin polymer film and then dried in a 30 °C vacuum oven for 12 h. No staining treatment was performed for the observation. SEM images were obtained with a field emission microscope (JEOL-6301F), which was operated with an accelerating voltage of 5 kV. All the samples prepared for SEM studies were coated with thin layers of gold (~15 nm in thickness) before the measurements.

2.5. Laser Light Scattering. Laser light scattering experiments were performed on a commercial LS instrument (ALV/DLS/SLS-5022F) equipped with a multi-τ digital time correlator (ALV/LSE-5003) and a solid-state laser (Uniphase, output power = 22 mW at λ = 632.8 nm). All measurements were carried out at 25 ± 0.1 °C. The dynamic light scattering (DLS) was used to determine the hydrodynamic radius (R_h) and polydispersity of the colloidal spheres and fractal aggregates formed in the aqueous media. For the measurements, the scattering angle was adjusted in range from 15° to 60°. The cumulant analysis was used to describe logarithm of the first-order electric field correlation function as a series expansion, where the first cumulant (Γ) yields the *z*-averaged diffusion coefficient and the second cumulant (μ_2) is a measure of polydispersity.[32] The Laplace inversion (CONTIN analysis) of the measured electric field correlation function can result in a line width distribution function $G(\Gamma)$. For a diffusive relaxation, Γ is related to the translational diffusion coefficient by $\Gamma = Dq^2$, where D is the translation diffusion coefficient, q [$= (4\pi n/\lambda_0)\sin(\theta/2)$] is the scattering vector, θ is the scattering angle, n is the refractive index of the solvent, and λ_0 is the wavelength of the incident light. $G(\Gamma)$ obtained at different scattering angles was converted to a hydrodynamic radius distribution $f(R_h)$, which was obtained by the CONTIN program equipped in the instrument. The translational diffusion coefficients were obtained from DLS by extrapolating to zero scattering angle. The average hydrodynamic radii ($\langle R_h \rangle$) were calculated from the diffusion coefficients based on the Stokes–Einstein equation.[33] The fractal dimensions (d_f) of the aggregates were determined by the static light scattering (SLS) measurement. For an aggregate with a fractal characteristics and formed by small particles, the scattered intensity $I(q)$ is scaled to q according to $I(q) \propto q^{-d_f}$ over the range of $R_{g,agg} > q^{-1} > R_{g,u}$, where $R_{g,agg}$ and $R_{g,u}$ are the radius of gyration for the aggregates and unimers.[29,34–36] In this study, SLS data were analyzed over scattering angles of 15°–150°, corresponding to 3.45×10^{-3} nm^{-1} < q < 2.56×10^{-2} nm^{-1}. The fractal dimensions of the aggregates were obtained from the slope of $I(q)$ versus q on a double-logarithmic plot.

2.6. Photoisomerization Analysis. The photoisomerization of the azo chromophores was induced by irradiation with UV light, which was from a high-intensity 365 nm UV lamp equipped with 12.7 cm diameter filter (Cole-Parmer L-97600-05 long wave UV lamp, U-09819-23 filter). The light intensity of the lamp was 7000 mW/cm^2 at a distance of 38 cm and 21 000 mW/cm^2 at a distance of 5 cm. The samples were placed at ca. 15 cm away from the lamp. The surrounding temperature of the samples was controlled to be about 30 °C by a cold plate. The UV–vis spectra of the samples were measured over different irradiation time intervals by using a Perkin-Elmer Lambda Bio-40 spectrophotometer. To study the effect of pH on photoresponsive behavior, the aqueous dispersions with different pH values were irradiated with the 365 nm UV light, and the UV–vis spectra were recorded over different time intervals until the photostationary states were achieved.

3. RESULTS AND DISCUSSION

Poly(2-(4-(phenylazo)phenoxy)ethyl acrylate-*co*-acrylic acid) (PPAPE), with the chemical structure given in Figure 1, was used as a representative amphiphilic random azo copolymer for this study. PPAPE was obtained by the reaction between a reactive precursor polymer (poly(acryloyl chloride), PAC) and 2-(4-(phenylazo)phenoxy)ethanol (PAPE) and the following hydrolysis of the unreacted acyl chloride groups to yield the carboxylic groups.[31] PPAPE is an amphiphilic copolymer composed of hydrophilic acrylic acid units and hydrophobic azobenzene-containing acrylate units. Because of the synthetic method, the hydrophobic units are randomly distributed along the polymeric chain and the polymer possesses polydispersity in both the molecular weight and the loading density of the hydrophobic units. The degree of functionalization (DF) is defined as the percentage amount of azobenzene units among total units. The PPAPE sample used in this study has the DF of 49.9%. The number-average molecular weight (M_n) and weight-average molecular weight (M_w) are 6.53×10^4 and 1.24×10^5, respectively. Our previous study shows that PPAPE can form uniform colloidal spheres through gradual hydrophobic aggregation of the polydispersed polymeric chains in THF–H_2O media as induced by a continuous increase in the water content.[16d] The colloidal spheres formed by this process have a hydrophobic core and hydrophilic corona. Results reported in the following parts

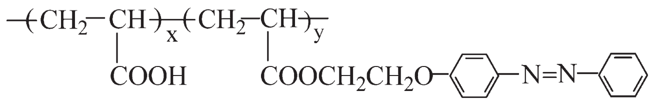

PPAPE

Figure 1. Chemical structure of PPAPE.

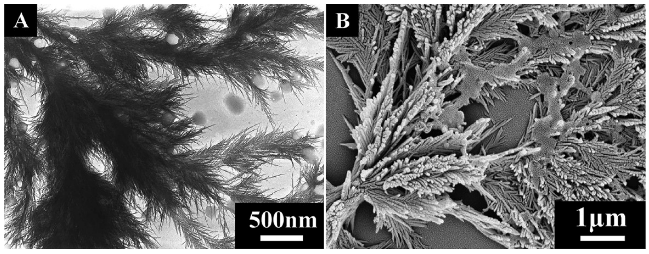

Figure 2. Typical TEM and SEM images of the fractal aggregates of PPAPE formed in the aqueous dispersions: (A) TEM image, pH = 9.4; (B) SEM image, pH = 8.8.

will show that, by gradual addition of the NaOH aqueous solution into the dispersion, the colloidal spheres do not undergo a simple disaggregation with the pH increase but transform into some highly organized fractal aggregates in the dispersions.

3.1. Fractal Structure Formation and Morphology. The colloidal spheres of PPAPE were prepared by dissolving PPAPE in THF and then gradually adding water into the solution. In a typical process, PPAPE was dissolved in THF to obtain a homogeneous solution with the polymer concentration of 0.8 mg/mL, and then Milli-Q water was gradually added into the THF solution. After the water content reached 50 vol %, the formed colloids were "quenched" by adding an excess amount of water, and the dispersion was dialyzed against water to remove THF. The colloidal spheres with an average hydrodynamic radius ($\langle R_h \rangle$) of 116 nm were obtained. The dispersion of colloidal spheres was weakly acidic (pH = 5.2) and had a concentration of 4.0×10^{-5} g/mL. The fractal aggregates were obtained by gradually adding the NaOH aqueous solution (0.2 M) into the dispersions of colloidal spheres to a proper pH value. Each time, 5–30 μL of NaOH solution was added into the dispersions (3 mL), and then the dispersions were set aside for 5–10 h to reach the pH stable state. The operation was repeated to obtain a series of dispersions with different pH values until the final pH value was obtained.

Figure 2A gives a typical TEM image of aggregates of PPAPE separated from the aqueous dispersion (pH = 9.4). The aggregates appear as needle-shaped leaves of pine tree growing in well-organized clusters. Figure 2B shows a typical SEM micrograph of the aggregates obtained from the dispersion with pH of 8.8. Although the aggregates on silicon wafer were coated with a thin layer of gold (~15 nm in thickness) for the SEM observation, the dendritic morphology can be clearly identified as that observed by the TEM. A close examination of the TEM image reveals that the aggregates are not constructed with the original colloidal spheres because the finest branches have a diameter of 10–20 nm, which is much smaller than the size of the initial colloidal spheres ($\langle R_h \rangle$ = 116 nm). Figure 3 gives the hydrodynamic diameter (D_h) and its distribution of PPAPE in THF solution, determined by dynamic light scattering (DLS). The average hydrodynamic diameter ($\langle D_h \rangle$) of a single chain coil of PPAPE is 15.6 nm. It indicates that the size of the finest branches is close to the dimensions of a single polymer chain or aggregates of few chains.

To study the morphology evolution in the process as well as the fractal characteristics of the formed aggregates, the aggregates formed in the dispersions with different pH values were separated for TEM observation. Figure 4A−I shows the morphological transformation from spherical colloids to the fractal aggregates when pH of the dispersions changes from 5.8 to 11.7. Figure 4A shows that the morphology remains as the original colloidal spheres at low pH (pH < 6). When pH is increased to 7−8, some colloidal spheres begin to dissociate from the shells to show the star-ramified morphology (Figure 4B,C). The ramified particles tend to associate with each other to form a larger cluster, where partially dissociated particles can still be seen but are connected with each other by some hairy structures. As indicated in our previous article, the colloidal spheres possess a hydrophobic core and hydrophilic corona.[16d] By increasing pH with the NaOH solution, the ionization of carboxyl groups of polymer at colloidal shells will cause partially dissociation of the polymeric chains from the corona as a result of the increased hydrophilicity. At this stage, the disaggregation mainly occurs at the colloidal shells and the hydrophobic cores almost remain unaffected. At higher pH (pH = 8.2, 8.5), remains of the colloidal spheres can still be seen and the aggregates develop to fine branches with dendritic structures (Figure 4D−F). When pH is increased to 9.4, the structures with many fine needle-shaped branches can be seen in the whole field of vision (Figure 4G). At even higher pH (pH = 10.6, 11.7), the clusters further transform into morphology similar to overlapping leaves of cypress with petioles and stems (Figure 4H,I). The TEM micrographs evidence that polymer chains in colloidal spheres gradually disassemble from the less hydrophobic shells to compact hydrophobic cores as the pH of the dispersion increases. During the process, the partially dissociated colloids gradually aggregate with each other to form the cluster structures. As the pH further increases, the formed clusters will undergo the structural reorganization to develop the clusters with finer branches.

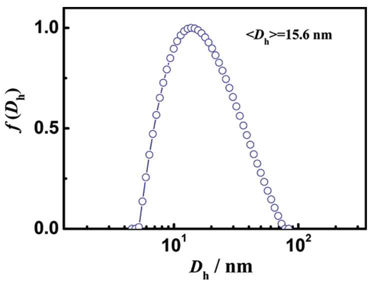

Figure 3. Hydrodynamic diameter (D_h) and its distribution of PPAPE in the THF solution. The average hydrodynamic diameter ($\langle D_h \rangle$) is 15.6 nm with the polydispersity index (PDI = $\mu_2/\langle\Gamma\rangle^2$) of 0.21.

3.2. Light Scattering Investigation. In order to understand the structure formation process in the dispersions, the static light scattering (SLS) was carried out to study the aggregate structures in the dispersions. SLS has been widely used to investigate structural self-similarity and determine the fractal dimension (d_f) of the aggregates.[28−30,34−37] In dilute solution, the excess scattering intensity of the polymer is related to the solution

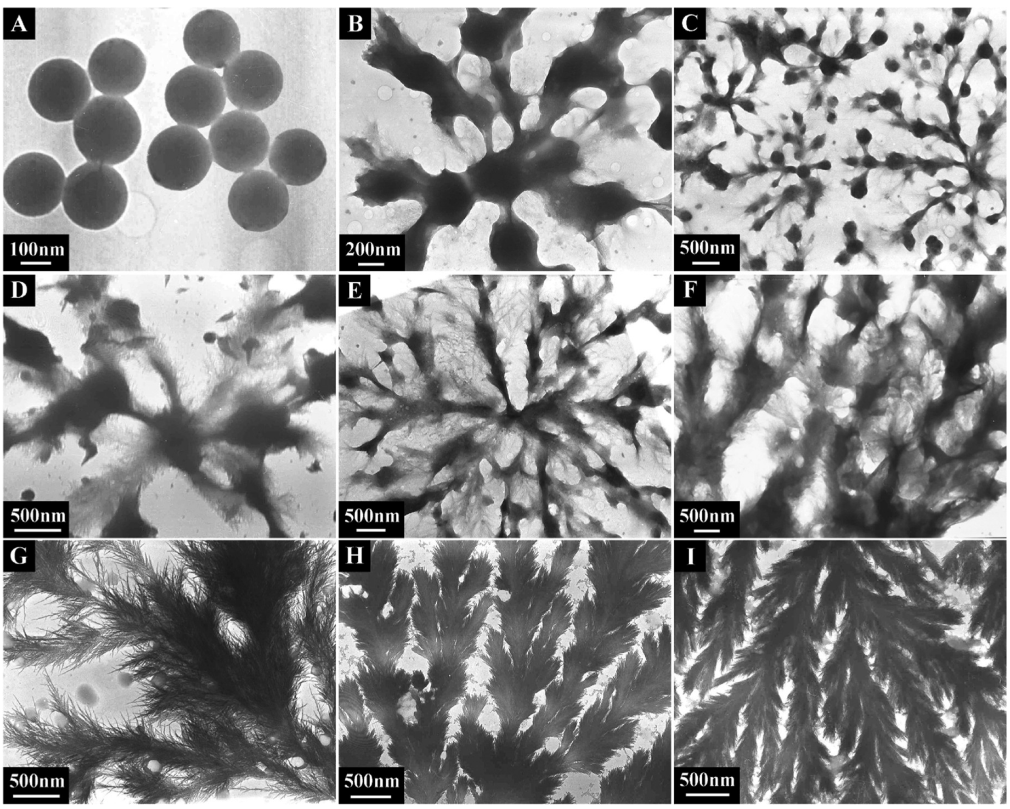

Figure 4. Typical TEM images of the colloidal spheres and fractal aggregates of PPAPE formed in the aqueous dispersions with the different pH values. (A) pH = 5.8, (B) pH = 7.5, (C) pH = 7.8, (D) pH = 8.2, (E, F) pH = 8.5, (G) pH = 9.4, (H) pH = 10.6, and (I) pH = 11.7.

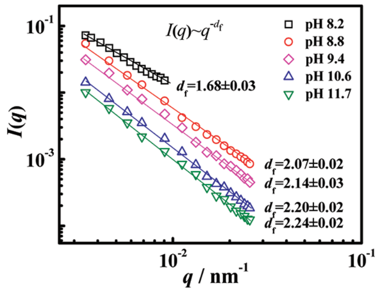

Figure 5. Plot of $I(q)$ versus q on a log−log coordinate for the aggregates in aqueous dispersions with pH in range 8.2−11.7.

structure factor $S(q)$ and the form factor $P(q)$

$$I(q) = (K/R_s)CM_wS(q)P(q) \tag{1}$$

where K is a constant factor, C is the polymer concentration, M_w is the polymer weight-average molecular mass, R_s is the solvent Rayleigh ratio, and q (= $(4\pi n/\lambda_0)\sin(\theta/2)$) is the scattering vector.[34,35] In eq 1, $S(q)$ and $P(q)$ reflect space correlation between polymer segments belong to different polymers and the same polymer. For the system studied here, the aggregates are formed by partially decomposed colloidal spheres and polymeric chains. The light scattering can be attributed to the polymer segments or volume elements in the aggregates. When the length scale q^{-1} meets the condition $R_{g,agg} > q^{-1} > R_{g,u}$, where $R_{g,agg}$ and $R_{g,u}$ are the radius of gyration for the aggregates and unimers (primary particles), the scattering intensity $I(q)/C$ is only due to local space correlation between the polymer segments or volume elements in the aggregates.[35] For an aggregate with a fractal characteristics, the scattered intensity shows the power-law dependence as follows:

$$I(q) = (K/R_s)CM_{app}(qR_{app})^{-d_f} \tag{2}$$

$$M_{app} \sim (R_{app})^{d_f} \tag{3}$$

where d_f is the fractal dimension and M_{app} and R_{app} are apparent mass and apparent radius.[35] The fractal dimension of the aggregates can be obtained from the $I(q) \sim q^{-d_f}$ relationship[28−30,34−37] and $M_w \sim (R_g)^{d_f}$ relationship.[34,38,39]

In this study, the fractal dimensions were obtained from the slope of $I(q)$ versus q on a double-logarithmic plot. Figure 5 shows the plots of $I(q)$ versus q on a log−log coordinate for aggregates formed in the dispersions with pH 8.2−11.7. The linear relationship between log $I(q)$ and log q indicates that the aggregates formed in the dispersions possess the fractal structures, whose d_f increases as the dispersion pH is increased. At comparatively low pH (pH = 8.2), the fractal dimension is 1.68 ± 0.03, which is close to a diffusion-limited cluster aggregation (DLCA) case. For this pH value, as the unimers are partially dissociated colloidal particles, the scattering angle can only be limited in the range from 15° to 40° to meet the condition $q^{-1} > R_{g,u}$. From the d_f value, it is believed that the partially dissociated particles aggregate with each other to form clusters according to the DLCA mechanism. The DLCA ("fast" aggregation) assumes that the particles stick to the growing cluster once encounter it (irreversible sticking), which leads to open and loose aggregates with d_f of 1.7−1.8 for a three-demensional (3D) system. When the pH values increase to 8.8 and 9.4, the d_f increases to 2.07 ± 0.02 and 2.14 ± 0.03, which show characteristics similar to a reaction-limited cluster aggregation (RLCA) process. An RLCA process corresponds to a "slow" aggregation, where the particles need several collisions to stick to the aggregates. RLCA usually produces fractals with a denser morphology and a higher d_f (2.1−2.2) for a 3D system because the components can penetrate into the growing clusters. When the pH values further increase to 10.6 and 11.7, the d_f increases to 2.20 ± 0.02 and 2.24 ± 0.02. In the process when the pH values increase from 8.2 to 9.4, the abruptly increased d_f indicates that the aggregation undergoes a mechanism transition from DLCA to RLCA. The structures observed by TEM (Figure 4G−I) correspond to the fractals formed through a process with d_f similar to the RLCA.

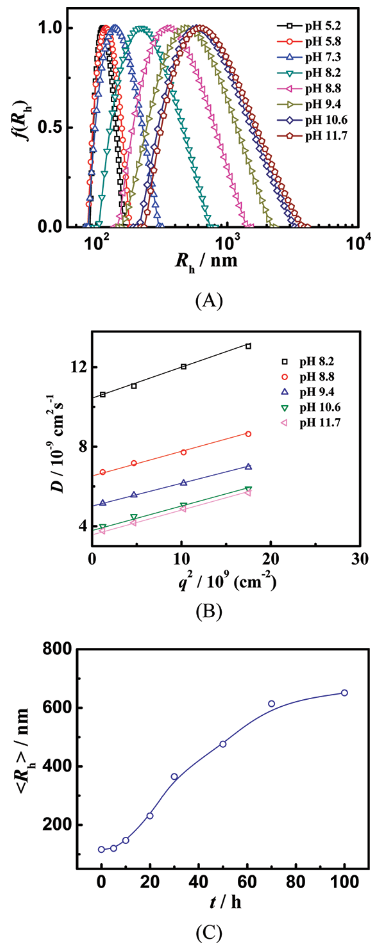

Figure 6. (A) The hydrodynamic radius (R_h) distribution of the aggregates formed at the different stages and obtained at the scattering angle of 15°; (B) extrapolation of the apparent diffusion coefficients toward zero for the scattering vector q; (C) relationship between the average hydrodynamic radius ($\langle R_h \rangle$) of aggregates and time.

The dynamic light scattering (DLS) can supply further information about the aggregate formation. As mentioned above, the aggregate formation process was controlled by adjusting the pH values of the medium with the addition of the NaOH solution into the dispersion. After one addition, the dispersion was set aside for a period of time. A series of dispersions with pH in range from 5.8 to 11.7 were obtained by this dynamic evolution process. The hydrodynamic radius (R_h) and polydispersity of aggregates formed in the aqueous dispersions were monitored by DLS after each time interval. Figure 6A gives R_h distributions of aggregates formed at the different stages, which were measured at the scattering angle of 15°. The distributions obtained at other scattering angles are given in the Supporting Information (Figures S1−S5). In diluted dispersion, the z-averaged diffusion coefficients (D) and apparent diffusion coefficient (D_{app}) have the following relationship:[34]

$$D_{app}(q) = D(1 + K\langle R_g^2\rangle_z q^2) \quad (4)$$

The "true" D values can be estimated by extrapolating the apparent diffusion coefficients toward zero for the scattering vector q. Under this condition, nondiffusional processes like rotation or polymer segment fluctuations will not contribute to the correlation function.[34] Figure 6B gives the extrapolation of the diffusion coefficients for the dispersions with the different pH values. The average hydrodynamic radii ($\langle R_h\rangle$) were calculated from the extrapolated diffusion coefficients based on the Stokes−Einstein equation. Figure 6C shows the variation of $\langle R_h\rangle$ with the time in the aggregate formation process. At the initial stage, where the dispersion pH is at the comparatively low side (pH = 5.2−7.3), $\langle R_h\rangle$ exhibits a very slow increase with the time increase. It corresponds to two simultaneous processes, i.e., the partial dissociation of the colloidal spheres and the aggregation of the partially dissociated particles. When time increases from 10 to 80 h (pH increases from 8 to 10), a sharp increase of $\langle R_h\rangle$ can be seen. The polydispersity index (PDI = $\mu_2/\langle\Gamma\rangle^2$) of aggregates, obtained at scattering angle of 15°, also exhibits a significant increase with the growth of the aggregate size (Table 1), where the pH values measured at the corresponding stages are also given. The rapid increase in $\langle R_h\rangle$ indicates that the sizes of the clusters significantly increase in the process. When the time further increases, corresponding to the pH increase to 11.7, $\langle R_h\rangle$ of the aggregates grows with a slow increasing rate. This stage reflects the near-equilibrium characteristic of the fractal growth.

Table 1. DLS Experimental Results of Aggregates Formed in the Dispersions at the Different Stages

NaOH (μL)	dispersion pH	$\langle R_h\rangle^a$ (nm)	$\mu_2/\langle\Gamma\rangle^{2\ b}$
0	5.2	116	0.027
5	5.8	120	0.036
20	7.3	147	0.094
40	8.2	236	0.17
80	8.8	372	0.23
150	9.4	487	0.25
240	10.6	629	0.28
330	11.7	676	0.29

[a] $\langle R_h\rangle$ was obtained by extrapolation of the apparent diffusion coefficients to zero for the scattering vector. [b] $\mu_2/\langle\Gamma\rangle^2$ is the polydispersity index of the aggregates dispersed in the water, measured by DLS at the scattering angle of 15°.

3.3. Photoisomerization Analysis. Photoisomerization behavior of azobenzene is sensitive to the local environment surrounding it. The property can be used as a tool to extract information about the local structures around the molecular probe.[40−42] To carry out the study, the dispersions of aggregates with different pH values were irradiated with 365 nm UV light for different time periods, and the UV−vis spectra of the samples were recorded until the photostationary states were achieved. Figure 7 shows the UV−vis spectra of the dispersions of the initial colloidal spheres (Figure 7A) and the fractal aggregates formed in dispersions with the different pH values (Figure 7B−D). For all the cases, the light irradiation causes a gradual decrease of the absorbance of the $\pi-\pi^*$ transition band at 360 nm and slight increase of the $n-\pi^*$ transition band at 450 nm as the result of the trans-to-cis isomerization of the azobenzene units.[2] From the figures, the absorbance at 360 nm before the light irradiation (A_{origin}) and the absorbance at the same wavelength after the irradiation for different time periods (A_t) can be obtained.

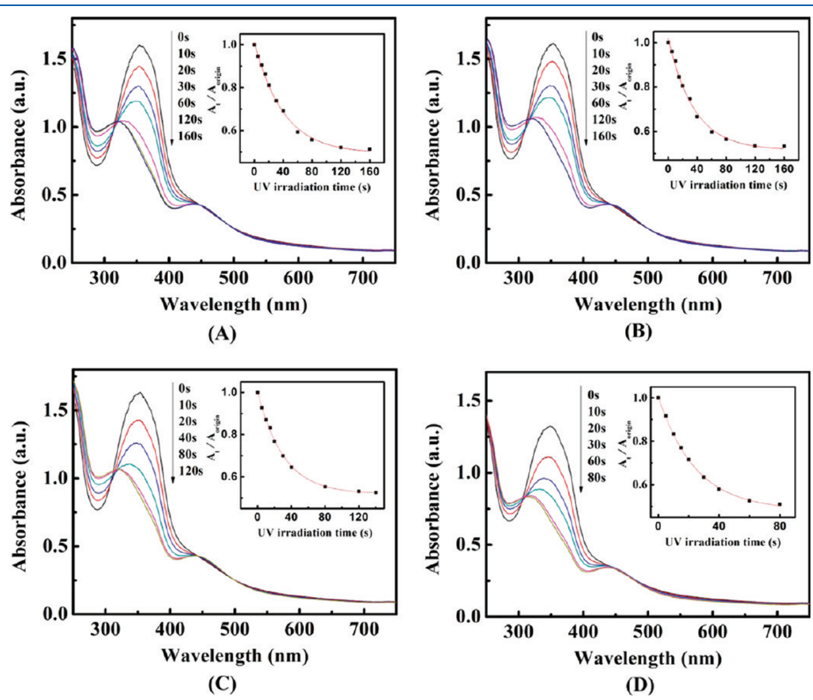

Figure 7. Variation of the UV−vis spectra of the dispersions induced by the UV light irradiation: (A) the colloidal sphere dispersion (pH = 5.2), (B−D) the fractal aggregate dispersions, pH = 8.5, 9.4, and 11.7. Inset: the relative absorbance (A_t/A_{origin}) varying with the irradiation time and the fitting curves.

Table 2. Coefficients of the Photoisomerization Kinetics Obtained from the Curve Fitting for the PPAPE Colloidal Spheres and Fractal Aggregates in Dispersions with the Different pH Values

dispersion pH	A_0	A_1	T_1 (s)	$\chi^{2\,a}$
5.2[b]	0.49	0.52	40.3	1.13×10^{-4}
8.5	0.52	0.50	35.7	2.13×10^{-4}
9.4	0.52	0.49	30.9	4.64×10^{-5}
11.7	0.48	0.52	24.4	3.20×10^{-5}

[a] Here χ^2 is the mean-squared error of the fitting. [b] The initial colloidal spheres.

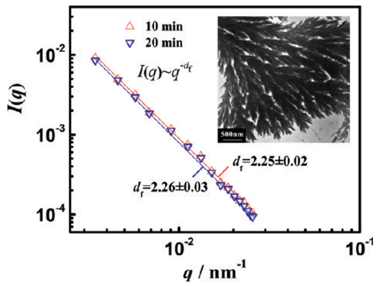

Figure 8. Plot of $I(q)$ versus q on a log−log coordinate obtained for the fractal aggregates after the UV light irradiation for 10 and 20 min (pH = 11.7). Inset: typical TEM image of the aggregates after the UV irradiation for 20 min (pH = 11.7).

The relative absorbance (A_t/A_{origin}) of the samples is used to characterize the relative amount of the trans isomers remaining at t time and the variations of A_t/A_{origin} with t represent the kinetics of the photoisomerization. The variations obtained from the experiments can be best fitted by the first-order exponential decay function

$$A_t/A_{origin} = A_0 + A_1 \exp(-t/T_1) \tag{5}$$

where T_1 is the characteristic time of the decay process. Both experimental data and fitting curves are correspondingly given as insets in Figure 7A−D. The coefficients obtained from the fitting are given in Table 2. Two extreme T_1 values obtained from the curve fitting are 40.3 and 24.4 s for the colloidal sphere (pH = 5.2) and fractal aggregate (pH = 11.7), respectively. The latter has an obviously smaller T_1 compared with the colloidal sphere, which means that the trans-to-cis isomerization rate is much faster for the fractal aggregate. It can also be seen from Table 2 that the characteristic time T_1 gradually decreases as the dispersion pH increases.

The above result can have two possible explanations; i.e., the fractal structures have large free volume around the azobenzene moieties, or the light irradiation causes the dissociation of the fractals. In order to figure out the exact occurrence, the SLS study was carried out before and after the light irradiation. Figure 8 shows the plot of $I(q)$ versus q on a log−log coordinate obtained for aggregates after the UV irradiation for 10 and 20 min (pH = 11.7). TEM micrograph of aggregates after the UV irradiation for 20 min is shown as the inset in the figure. The log $I(q)$ versus log q plotting is straight lines, which indicates that even after 20 min irradiation, fractal structures still exist in the dispersion. The TEM observation also confirms the existence of fractal aggregates. The values of d_f obtained from the lines are 2.25 ± 0.02 and 2.26 ± 0.03 for aggregates after the UV light irradiation for 10 and 20 min, which are almost the same as the value before the light irradiation (d_f = 2.24 ± 0.02). The result of the photoisomerization study suggests that there is larger free volume around the azobenzene units in the fractal structures than in the colloidal spheres. SLS results given in section 3.2 indicate that when aggregation changes from DLCA to RLCA, the fractals became denser look at the large scale. On the other hand, the decrease of T_1 with the dispersion pH increase indicates that the structure obtained from RLCA is actually looser at the molecular level in the agglomerates.

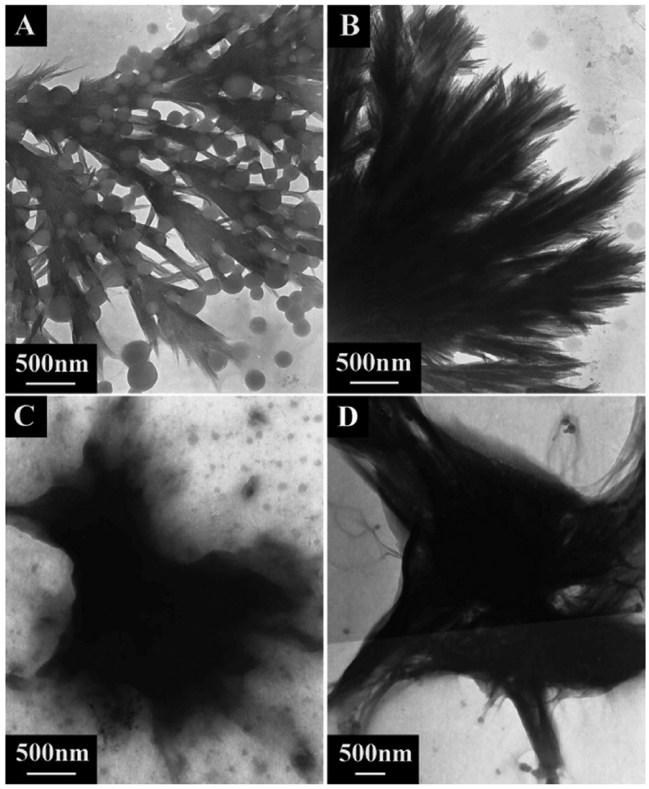

Figure 9. TEM images of the aggregates of PPAPE obtained under different conditions. (A) and (B) aggregates obtained by once adding the 0.2 M NaOH solutions into the dispersions of colloids to reach pH = 8.7 and pH = 10.8; (C) and (D) aggregates formed by adding the 0.2 M NaOH aqueous solution dropwise into the THF solutions of PPAPE and then added the deionized water into the solutions, (C) pH = 9.7, (D) pH = 11.1.

3.4. Influences of Other Preparation Conditions. The unique fractal structure formed at high pH (such as pH ∼ 9 and above) is closely related with the way to add the NaOH solution into the aqueous dispersions of the colloidal spheres. Figure 9A,B shows the TEM images of the aggregates obtained by once adding the total amount of the required NaOH solution into the dispersions of colloids. At both the low pH (pH = 8.7) and high pH (pH = 10.8), the morphology observed (Figure 9A,B) is obviously different with those shown in Figure 4. Although some fractal characteristics can be identified, the structures are not well developed. It is consistent with the DLS result given above, which further confirms that the procedure to gradually increase pH is critical for the slow fractal formation process. Moreover, if the NaOH solution was first dropwise added into the THF solutions of the azo polymers and then H_2O was slowly added into the THF solutions, only some ill-defined structures can be obtained (Figure 9C,D). In this case, the building blocks are mainly the polymer chains dissolved in the THF solutions. It indicates that the aggregation of the partially dissociated colloidal spheres at the initial stage is important for the formation of the well-organized structures in the high-pH dispersions.

3.5. Discussion. The above results indicate that the amphiphilic random azo copolymers can form a series of well-organized fractal structures related with the pH and preparation conditions. The scenario of the structure formation can be described as follows. At low pH side (pH = 8.2), the partially dissociated colloid spheres are the main component of the building blocks, which aggregate through DLCA process to form the clusters. At higher pH (such as pH ∼ 9), as the NaOH solution was added into dispersions in a very slow rate, the pH undergoes a gradual increase to reach the final value through the intermediate stages. In the intermediate stages, the partially dissociated colloid spheres first aggregate to form the fractal clusters. As the pH is increased, more and more polymer chains are dissociated from the colloidal particles and assemble to form the finer structures on the clusters. Owing to the electrostatic repulsion of the ionized carboxylic groups, polymeric chains take the more extended conformation at high pH and are difficult to associate with each other through the hydrophobic interaction. Therefore, the aggregation undergoes a mechanism transition from simple aggregation to the structural reorganization, which yields fractals with d_f similar to a RLCA process. At high pH side (pH = 10.6 and 11.7), the structural reorganization is further enhanced, which leads to the dense-look fractal structures (Figure 4H−I). The slow increase of pH with time is a very important control factor, which enable the polymeric chains to assemble in the process. The needlelike structures given in Figure 2A, obtained in dispersion with the intermediate pH value (pH ∼ 9), reflect the delicate balance between the colloid aggregation and structural reorganization.

4. CONCLUSION

This study shows for the first time that a series of fractal structures can be obtained from an amphiphilic random azo copolymer (PPAPE). The fractals were obtained by gradually adding the NaOH solution into aqueous dispersions of colloidal spheres of PPAPE. By adjusting pH of the aqueous dispersions, fractal aggregates with the different fractal dimensions (d_f) and morphology were obtained. In the low pH range (such as pH = 8.2), the fractals formed by the aggregation of the partially dissociated colloidal spheres through a DLCA process. At the high pH side (such as pH ∼ 9 and above), fractal structures with pine-needle-shaped and cypress-leaves-like morphology were obtained, which had d_f in the RLCA regime. The investigation with TEM, LLS, and photoisomerization suggested that the well-organized fractal structures obtained at high pH (pH ∼ 9 and above) were formed through the colloidal sphere aggregation and the subsequent structural reorganization. The slow increase of pH with time played a key role in the process. The observations reported here can supply a better understanding of the molecular self-assembling nature and be used to develop photoresponsive materials with better performance.

■ ASSOCIATED CONTENT

Supporting Information. Figures S1−S5. This material is available free of charge via the Internet at http://pubs.acs.org.

■ AUTHOR INFORMATION

Corresponding Author

*E-mail: wxg-dce@mail.tsinghua.edu.cn. Tel: 86-10-62784561. Fax: 86-10-62770304.

■ ACKNOWLEDGMENT

The financial support from the NSFC under Project 91027024 is gratefully acknowledged.

■ REFERENCES

(1) Delaire, J. A.; Nakatani, K. *Chem. Rev.* **2000**, *100*, 1817–1845.

(2) Natansohn, A.; Rochon, P. *Chem. Rev.* **2002**, *102*, 4139–4175.

(3) Ikeda, T.; Mamiya, J. I.; Yu, Y. L. *Angew. Chem., Int. Ed.* **2007**, *46*, 506–528.

(4) Ikeda, T.; Horiuchi, S.; Karanjit, D. B.; Kurihara, S.; Tazuke, S. *Macromolecules* **1990**, *23*, 42–48.

(5) Todorov, T.; Nikolova, L.; Tomova, N. *Appl. Opt.* **1984**, *23*, 4309–4312.

(6) (a) Finkelmann, H.; Nishikawa, E.; Pereira, G. G.; Warmer, M. *Phys. Rev. Lett.* **2001**, *87*, 015501. (b) Yu, Y. L.; Nakano, M.; Ikeda, T. *Nature* **2003**, *425*, 145. (c) Li, M. H.; Keller, P.; Li, B.; Wang, X. G.; Brunet, M. *Adv. Mater.* **2003**, *15*, 569–572. (d) Hosono, N.; Kajitani, T.; Fukushima, T.; Ito, K.; Sasaki, S.; Takata, M.; Aida, T. *Science* **2010**, *330*, 808–811.

(7) (a) Camacho-Lopez, M.; Finkelmann, H.; Palffy-Muhoray, P.; Shelley, M. *Nature Mater.* **2004**, *3*, 307–310. (b) Yamada, M.; Kondo, M.; Mamiya, J.; Yamada, M.; Yu, Y. L.; Kinoshita, M.; Barrett, C. J.; Ikeda, T. *Angew. Chem., Int. Ed.* **2008**, *47*, 4986–4988. (c) Yoshino, T.; Kondo, M.; Mamiya, J.; Kinoshita, M.; Yu, Y. L.; Ikeda, T. *Adv. Mater.* **2010**, *22*, 1361–1363.

(8) (a) Rochon, P.; Batalla, E.; Natansohn, A. *Appl. Phys. Lett.* **1995**, *66*, 136–138. (b) Kim, D. Y.; Tripathy, S. K.; Li, L.; Kumar, J. *Appl. Phys. Lett.* **1995**, *66*, 1166–1168.

(9) (a) Hugel, T.; Holland, N. B.; Cattani, A.; Moroder, L.; Seitz, M.; Gaub, H. E. *Science* **2002**, *296*, 1103–1106. (b) van Oosten, C. L.; Bastiaansen, C. W. M.; Broer, D. J. *Nature Mater.* **2009**, *8*, 677–682. (c) Ohm, C.; Brehmer, M.; Zentel, R. *Adv. Mater.* **2010**, *22*, 3366–3387.

(10) (a) Zhao, Y.; He, J. *Soft Matter* **2009**, *5*, 2686–2693. (b) Yagai, S.; Kitamura, A. *Chem. Soc. Rev.* **2008**, *37*, 1520–1529.

(11) (a) Tian, Y. Q.; Watanabe, K.; Kong, X. X.; Abe, J.; Iyoda, T. *Macromolecules* **2002**, *35*, 3739–3747. (b) Yu, H. F.; Iyoda, T. *J. Am. Chem. Soc.* **2006**, *128*, 11010–11011.

(12) Wang, G.; Tong, X.; Zhao, Y. *Macromolecules* **2004**, *37*, 8911–8917.

(13) Wang, D. R.; Ren, H. F.; Wang, X. Q.; Wang, X. G. *Macromolecules* **2008**, *41*, 9382–9388.

(14) del Barrio, J.; Oriol, L.; Sánchez, C.; Serrano, J. L.; Cicco, A. D.; Keller, P.; Li, M. H. *J. Am. Chem. Soc.* **2010**, *132*, 3762–3769.

(15) Tsuda, K.; Dol, G. C.; Gensch, T.; Hofkens, J.; Latterini, L.; Weener, J. W.; Meijer, E. W.; De Schryver, F. C. *J. Am. Chem. Soc.* **2000**, *122*, 3445–3452.

(16) (a) Li, Y. B.; He, Y. N.; Tong, X. L.; Wang, X. G. *J. Am. Chem. Soc.* **2005**, *127*, 2402–2403. (b) Li, Y. B.; Deng, Y. H.; He, Y. N.; Tong, X. L.; Wang, X. G. *Langmuir* **2005**, *21*, 6567–6571. (c) Li, Y. B.; Tong, X. L.; He, Y. N.; Wang, X. G. *J. Am. Chem. Soc.* **2006**, *128*, 2220–2221. (d) Li, Y. B.; Deng, Y. H.; Tong, X. L.; Wang, X. G. *Macromolecules* **2006**, *39*, 1108–1115.

(17) (a) Mandelbrot, B. B. *The Fractal Geometry of Nature*; W. H. Freeman: San Francisco, CA, 1982. (b) Mandelbrot, B. B. *Fractals: Form, Chance, and Dimension*; W. H. Freeman: San Francisco, CA, 1977.

(18) Meakin, P. *Fractals, Scaling and Growth Far from Equilibrium*; Cambridge University: London, 1998.

(19) (a) Witten, T. A.; Sander, L. M. *Phys. Rev. Lett.* **1981**, *47*, 1400–1403. (b) Witten, T. A.; Sander, L. M. *Phys. Rev. B* **1983**, *27*, 5686–5697.

(20) Meakin, P. *Phys. Rev. Lett.* **1983**, *51*, 1119–1122.
(21) (a) Meakin, P. *Phys. Rev. A* **1990**, *41*, 2005–2020. (b) Meakin, P. *Adv. Colloid Interface Sci.* **1988**, *28*, 249–331. (c) Brown, W. D.; Ball, R. C. *J. Phys. A* **1985**, *18*, L517.
(22) Vicsek, T. *Fractal Growth Phenomena*; World Scientific: London, 1992.
(23) (a) Tirado-Miranda, M.; Schmitt, A.; Gallejas-Fernández, J.; Fernández-Barbero, A. *Langmuir* **1999**, *15*, 3437–3444. (b) Kim, A. Y.; Berg, J. C. *Langmuir* **2000**, *16*, 2101–2104.
(24) van Herrikhuyzen, J.; Janssen, R. A. J.; Meijer, E. W.; Meskers, S. C. J.; Schenning, A. P. H. J. *J. Am. Chem. Soc.* **2006**, *128*, 686–687.
(25) Goldys, E. M.; Drozdowicz-Tomsia, K.; Xie, F.; Shtoyko, T.; Matveeva, E.; Gryczynski, I.; Gryczynski, Z. *J. Am. Chem. Soc.* **2007**, *129*, 12117–12122.
(26) (a) Verheul, M.; Roefs., S. P. F. M.; Mellema, J.; de Kruif, K. G. *Langmuir* **1998**, *14*, 2263–2268. (b) Molina-Bolívar, J. A.; Galisteo-González, F.; Hidalgo-Álvarez, R. *Langmuir* **2001**, *17*, 2514–2520.
(27) (a) Rubinstein, M.; Dobrynin, A. V. *Trends Polym. Sci.* **1997**, *5*, 181–186. (b) Rubinstein, M.; Dobrynin, A. V. *Curr. Opin. Colloid Interface Sci.* **1999**, *4*, 83–87.
(28) Peng, S. F.; Wu, C. *Macromolecules* **1999**, *32*, 585–589.
(29) Dai, S.; Tam, K. C.; Jenkins, R. D. *Macromolecules* **2000**, *33*, 404–411.
(30) Lin, W.; Zhou, Y. S.; Zhao, Y.; Zhu, Q. S.; Wu, C. *Macromolecules* **2002**, *35*, 7407–7413.
(31) Wu, L. F.; Tuo, X. L.; Cheng, H.; Chen, Z.; Wang, X. G. *Macromolecules* **2001**, *34*, 8005–8013.
(32) Chu, B. *Laser Light Scattering*; Academic Press: New York, 1991.
(33) Berne, B.; Pecora, R. *Dynamic Light Scattering*; Plenum Press: New York, 1976.
(34) Schärtl, W. *Light Scattering from Polymer Solutions and Nanoparticle Dispersions*; Springer-Verlag: Berlin, 2007.
(35) Raspaud, E.; Lairez, D.; Adam, M.; Carton, J. P. *Macromolecules* **1994**, *27*, 2956–2964.
(36) Peng, S. F.; Wu, C. *Macromolecules* **2001**, *34*, 6795–6801.
(37) Janine, L. B.; Yan, Y. D.; Jameson, G. J.; Biggs, S. *Langmuir* **1997**, *13*, 6413–6420.
(38) Huber, K.; Witte, T.; Hollmann, J.; Keuker-Baumann, S. *J. Am. Chem. Soc.* **2007**, *129*, 1089–1094.
(39) Lages, S.; Michels, R.; Huber, K. *Macromolecules* **2010**, *43*, 3027–3035.
(40) Williams, J. L. R.; Daly, R. C. *Prog. Polym. Sci.* **1977**, *5*, 61–93.
(41) Kumar, G. S.; Nechers, D. C. *Chem. Rev.* **1989**, *89*, 1915–1925.
(42) Chaibundit, C.; Ricardo, N. M. P. S.; Crothers, M.; Booth, C. *Langmuir* **2002**, *18*, 4277–4283.